Inhibition of Tryptophan on AA 2024 in Chloride-Containing Solutions

Xing Li, Bin Xiang, Xiu-li Zuo, Qin Wang, and Zi-dong Wei

The inhibitory effects of tryptophan on the corrosion of AA 2024 in 1 M HCl, 20% (wt.%) CaCl$_2$, and 3.5% (wt.%) NaCl solutions were investigated via polarization techniques, electrochemical impedance spectroscopy, and weight loss methods. The scanning electron microscope technique was employed to observe corrosion morphology. The results suggest that AA 2024 was corroded in these three corrosive media to some extent and that tryptophan can significantly inhibit the corrosion of aluminum alloys. The inhibition efficiency (η) increased with increasing concentrations of tryptophan, and the best inhibition efficiency exhibited was about 87% in 1 M HCl solution with 0.008 M tryptophan. Tryptophan acted as a cathodic corrosion inhibitor and affected the hydrogen evolution reaction, which was the main electrode reaction in the 1 M HCl solution. In solutions with 20% CaCl$_2$ and 3.5% NaCl, tryptophan was adsorbed onto anodic areas, thus increasing the activation energy of the interface reaction as an anodic corrosion inhibitor. The Dmol^3 program of Material Studio 4.0 was used to obtain the optimized geometry of the tryptophan inhibitor and some quantum-chemical parameters. Front orbital distributions and Fukui indices indicate that the molecular active reaction zones were located in the indole ring of tryptophan.

1. Introduction

Aluminum alloys have remarkable economic and industrial importance, due mainly to their low cost, light weight, and high thermal, and electrical conductivity. They have many applications in the construction, transportation, and light industries, and they are used for civil purposes as well. The most important feature of aluminum is its resistance to corrosion due to its capability to form a protective film on its surface upon exposure to the atmosphere or water (Ref 1). This corrosion resistance, however, easily deteriorates in acidic and basic media. The presence of halide ions in a medium, especially the chloride ion, is disadvantageous to aluminum and produces pitting in the oxide film, thus reducing its resistance to corrosion. The anticorrosion capability of aluminum alloys decreases significantly in seawater and marine atmosphere conditions (Ref 2-4). Aluminum and its alloys are widely used in heat exchange equipment, condensers, air coolers, crystallisers, reactors, desiccators, tanks, tank cars, pipe works, etc. The environments in which these equipments operate are often moist, acid or alkaline, or contain other corrosive media, such as chloride ions. Hence, the corrosion of aluminum alloys is a serious problem and limits its application in the industry (Ref 5-8). Many environments in which aluminum alloys are employed contain chlorides. As such, the development of new

inhibitors that can effectively increase the corrosion resistance of aluminum in chloride environments is necessary. Unfortunately, many common corrosion inhibitors are hazardous to humans, difficult to degrade, and pollute the environment. In order to solve this problem, some researchers began to search for new green corrosion inhibitors to replace traditional ones. Most natural amino acids are alpha amino acids with extensive sources and biodegradability, and contain carboxyl and amino groups bonded to the same carbon atom. As corrosion inhibitors, amino acids have shown good performance (Ref 9-13). Ashassi-Sorkhabi (Ref 11) investigated the effects of alanine, glycine, and leucine against steel corrosion in HCl solutions and found that their inhibitory effects ranged from 28% to 91%. Oguzie (Ref 12) studied the corrosion inhibition of methionine (MTI) in mild steel in sulfuric acid and found that its inhibition efficiency increased with an increasing MTI concentration. This inhibition was further synergistically increased in the presence of KI, reaching an optimum [KI]/[MTI] ratio of 5/5. Kiani et al. (Ref 13) studied the inhibition effects of the amino acids cysteine, methionine, and alanine against the corrosion of lead-alloys (Pb-Ca-Sn) in H$_2$SO$_4$ solution and found that inhibition efficiency depended on the amino acid type and concentration. For example, the inhibition efficiency for 0.1 M cysteine in 0.5 M H$_2$SO$_4$ was greater than 96%. The molecular structure of tryptophan, presented in Fig. 1, shows a planar benzene ring and pyrrole ring, possessing Π bonds, and N, carboxyl, and amino groups. These are regarded as important factors for good inhibition.

In this study, the inhibition properties and effects of tryptophan in 1 M HCl, 20% CaCl$_2$, and 3.5% NaCl solutions were investigated. These media were selected to simulate several special application environments, such as those that are strongly acidic or that contain depassivator chloride ions. Weight loss measurements, polarization techniques, electrochemical impedance spectroscopy (EIS), and scanning electronic microscopy (SEM) were used to determine the inhibition

Xing Li, Bin Xiang, X. Zuo, Qin Wang, and Zi-dong Wei, College of Chemistry and Chemical Engineering, Chongqing University, Chongqing 400044, China. Contact e-mail: lixing03@126.com.
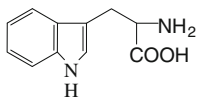
Fig. 1 Tryptophan molecule structure

efficiency of tryptophan. Quantum-chemical calculations were used to clarify the interaction between tryptophan molecules and the metal surface via a molecular orbital approach. Tryptophan is slightly soluble in water. In 20% CaCl₂ solution, however, it is difficult to dissolve. Thus, in this study, the tryptophan concentrations used were lower than 0.01 M.

2. Experimental Methods

2.1 Electrochemical Test

The material used for the study was AA 2024. For polarization studies, the specimens were mounted in epoxy resins, and only 1 cm^2 surface areas were exposed to corrosive media. A three-electrode cell, consisting of an aluminum working electrode (WE), a platinum counter electrode (CE), and a saturated calomel reference electrode (SCE), was used for the measurements. The surfaces of the WEs were polished with a sequence of emery papers from grades 300 to 1000, washed with distilled water, and then degreased with ethanol. The unstirred electrolytes used as corrosive media were a 1 M HCl solution, 20% CaCl₂ solution, and 3.5% NaCl solution, all of which had an absence and presence of different concentrations (0.0005, 0.005, and 0.008 M) of tryptophan. The electrodes were immersed into the solutions to establish steady-state open circuit potentials. The polarization and EIS experiments were carried out using an Autolab PGSTAT30 electrochemical analyser system (Eco Chemie BV, the Netherlands). The corrosion data of EIS were measured and analysed by frequency response analyser (FRA 4.9) software in the frequency range of 10 kHz to 0.01 Hz with 10 mV voltage amplitude of AC potential. Polarization curves were obtained and analysed via GPES software at a potential scan rate of 1 mV per second from low to high within the potential range of the open circuit potential ±150 mV.

2.2 Weight Loss Measurements and SEM Studies

Aluminum alloys with exposed surface areas of 4 cm^2 were used for the weight loss measurements. The samples were degreased with acetone, rinsed with distilled water, and then dried and weighed. They were then immersed into a 1 M HCl solution for 2 h, a 20% CaCl₂ solution for 72 h, and a 3.5% NaCl solution for 120 h. Afterward, the corrosion products on the metal surfaces were removed according to Chinese government standard GB10124-88 (Ref 14). The samples were again degreased with acetone, rinsed with distilled water, and then dried and weighed. Measurements were carried out in the absence and presence of different concentrations (0.0005, 0.005, and 0.008 M) of the inhibitor. Some samples with weight loss measurements were observed via SEM.

2.3 Quantum-Chemical Calculation

Theoretical calculations for the tryptophan molecule were performed using the Dmol^3 program of Material Studio 4.0.

The optimized geometry of the tryptophan molecule, the frontier molecular orbital surfaces, and the energies of the molecules were visualized.

3. Results and Discussion

3.1 Electrochemical Impedance Spectroscopy

Figure 2 shows the Nyquist plots of the aluminum alloys in 1 M HCl solution, 20% CaCl₂ solution, and 3.5% NaCl solution containing different concentrations of tryptophan.

In 1 M HCl solutions (Fig. 2a), the figure manifests one capacitive loop followed by an inductive loop. The capacitive loop may be attributed to the charge transfer resistance parallel to the double layer capacitance, which represents the corrosion rate of the aluminum alloy. Thus, the corrosion rate was reduced with increasing inhibitor concentrations. Either the oxidation film was damaged and became incomplete, or the intermediates and inhibitors were adsorbed onto and desorbed from the metal surface, thus leading to inductive loops (Ref 15-17). In 1 M HCl solutions, the inductive loop is attributed to the incomplete passive film caused by the faster dissolution, rather than growth, rate of the passive film.

In 20% CaCl₂ solutions (Fig. 2b), two capacitive loops exist. The loop at lower frequencies is associated with the Faradaic process occurring on the aluminum through defects and pores in the adsorbed inhibitor layer. The loop found at higher frequencies, on the other hand, corresponds to the resistance and capacitance of the oxidation film of the aluminum alloy. Figure 2(b) also shows that increasing the concentration of tryptophan also increases the impedance values of the aluminum alloy, further indicating that the inhibition effect increased. In particular, increases in its inhibitory effects were obvious when the concentration of tryptophan reached 0.005 M.

Only one capacitive loop is seen in 3.5% NaCl solutions (Fig. 2c), which is thought to be related to the double layer capacitance of the aluminum alloy surface. The radius of the capacitive loop increases with increasing inhibitor concentration. Thus, the reaction resistance increased, and the corrosion rate decreased.

3.2 Polarization

Figure 3 shows the polarization curves of aluminum in the three media at various concentrations of tryptophan. The corresponding corrosion data are given in Table 1. The following equation was used to calculate the inhibition efficiency (IE) from polarization measurements:

$$IE\% = (1 - i/i_0) \times 100, \qquad \text{(Eq 1)}$$

where i_0 and i represent the corrosion current density (A cm^{-2}) in the absence and presence of tryptophan, respectively. The inhibition efficiencies of tryptophan are given in Table 1. In general, the corrosion current density and corrosion rate decrease with increasing inhibitor concentrations. This is especially true for the 1 M HCl and 20% CaCl₂ solutions.

As shown in Fig. 3(a), with the increase in tryptophan concentrations, E_{corr} shifts toward more negative values, indicating that the cathode hydrogen evolution reaction was inhibited by tryptophan. In this case, tryptophan acted as a
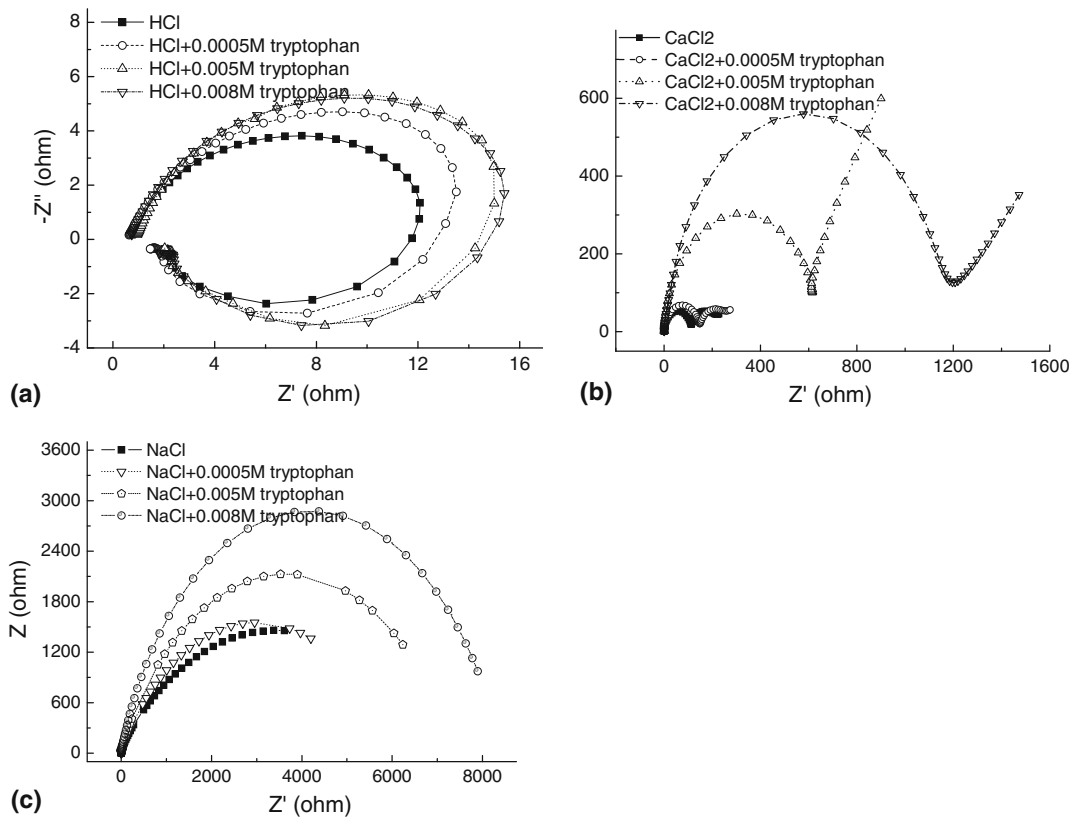
Fig. 2 Nyquist diagrams of the aluminum alloys in three solutions containing 0, 0.0005, 0.005, and 0.008 M tryptophan: (a) 1 M HCl; (b) 20% CaCl$_2$; and (c) 3.5% NaCl
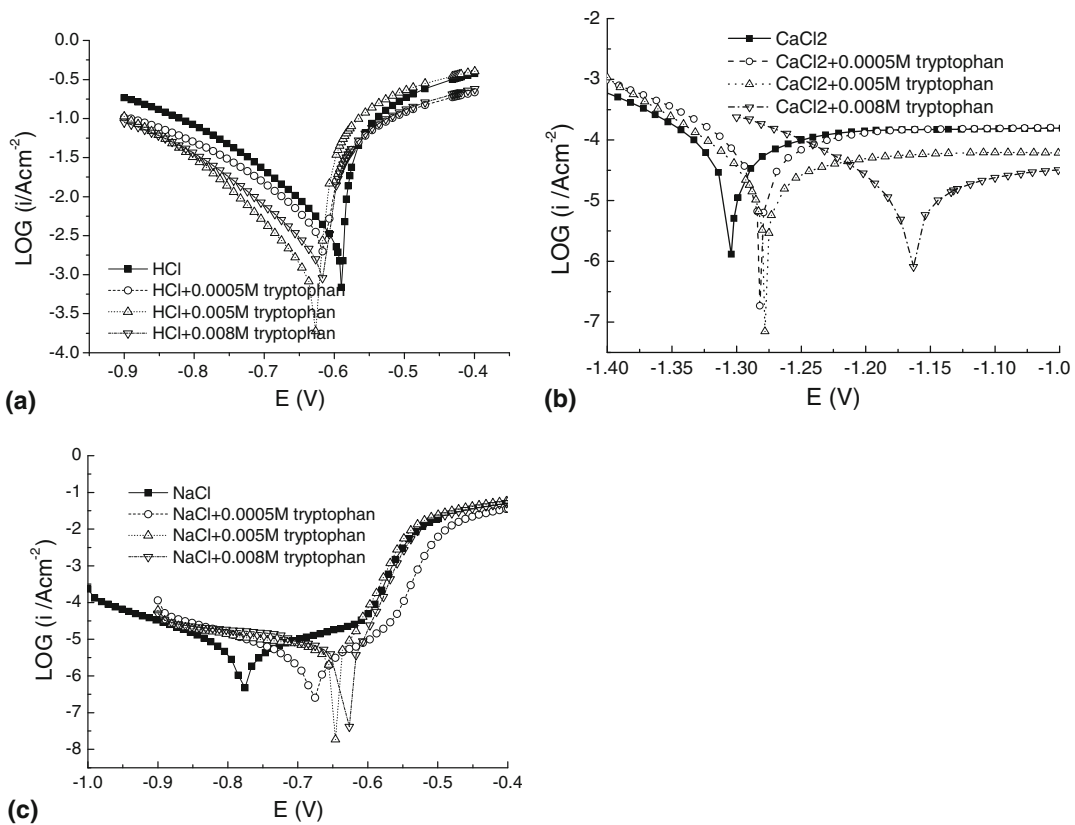

Fig. 3 Polarization curves of aluminum alloys in three solutions containing 0, 0.0005, 0.005, and 0.008 M tryptophan: (a) 1 M HCl, (b) 20% CaCl$_2$, and (c) 3.5% NaCl

Table 1 Corrosion parameters of aluminum alloys in 1 M HCl, 20% CaCl$_2$, and 3.5% NaCl containing different concentrations of tryptophan

Solution	Concentration of tryptophan, M	E_{corr}, V	I_{corr}, A cm^{-2}	$\eta\%$
1 M HCl	0	−0.589	6.403E−3	...
	0.0005	−0.613	4.296E−3	32.91
	0.005	−0.625	2.469E−3	61.44
	0.008	−0.612	7.445E−4	88.37
20% CaCl$_2$	0	−1.304	1.363E−4	...
	0.0005	−1.259	9.178E−5	32.66
	0.005	−1.278	4.195E−5	69.22
	0.008	−1.165	2.273E−5	83.32
3.5% NaCl	0	−0.779	3.954E−6	...
	0.0005	−0.679	2.24E−6	43.35
	0.005	−0.647	1.062E−6	73.14
	0.008	−0.627	7.688E−7	80.55

cathodic inhibitor. In the 20% CaCl$_2$ and 3.5% NaCl solutions, the cathodic process was predominantly controlled by oxygen reduction, and a slower corrosion rate is observed. In these cases, tryptophan was adsorbed onto anodic areas, thus increasing the activation energies of the interface reaction as an anodic corrosion inhibitor. As such, anodic reactions were affected.

3.3 Weight Loss Measurements and SEM Studies

The weight loss of the aluminum alloys in 1 M HCl, 20% CaCl$_2$, and 3.5% NaCl solutions in the presence and absence 0.0005, 0.005, and 0.008 M tryptophan was determined. Inhibition efficiency values were also calculated and are listed in Table 2. The inhibition efficiencies of tryptophan were calculated according to Eq 2:

$$\eta(\%) = (1 - W_{add}/W_{free}) \times 100, \qquad (Eq\ 2)$$

where W_{free} and W_{add} represent the weight loss of the samples due to dissolution in the three solutions without and with different concentrations of tryptophan, respectively. The inhibition efficiencies of tryptophan are given in Table 2. Corrosion rates were calculated according to Eq 3 (Ref 14):

$$R_r = (8.76\,W \times 10^7)/(ATD), \qquad (Eq\ 3)$$

where R is the corrosion rate (mm/a), W is the weight loss of the aluminum alloy in three solutions, and A, T, and D are the surface area (cm^2), immersion time (h), and density of the aluminum alloy (kg/m^3), respectively.

The data in Table 2 suggest that aluminum alloys have the fastest corrosion rate in 1 M HCl solutions, corrode slower in 20% CaCl$_2$ solutions, and corrode slowest in 3.5% NaCl solutions. Tryptophan acted as a good corrosion inhibitor for the aluminum alloys in these three solutions. The inhibition efficiency of tryptophan was observed to increase with increasing inhibitor concentration.

Figure 4 shows the surface appearance of the samples after immersion in three different types of corrosion media. Figure 4 also shows some differences on the microcorrosion morphology of the aluminum alloys after immersion. Large and deep corrosion pits were observed in Fig. 4(a), indicating that extensive corrosion occurred on the surface of the alloy in 1 M HCl. In the solution containing 20% CaCl$_2$ (Fig. 4c), several pits, many cracks, and some corrosion products were found, while only slight corrosion and some cracks were

Table 2 Corrosion parameters of tryptophan on aluminum corrosion in 1 M HCl, 20% CaCl$_2$, and 3.5% NaCl solutions obtained from weight loss measurements

Solution	Concentration of tryptophan, M	R, mm/a	$\eta\%$
1 M HCl	0	340.00	...
	0.0005	216.48	36.33
	0.005	87.76	38.00
	0.008	44.11	87.02
20% CaCl$_2$	0	0.245	...
	0.0005	0.158	35.51
	0.005	0.0788	67.84
	0.008	0.035	85.71
3.5% NaCl	0	0.0683	...
	0.0005	0.0420	38.49
	0.005	0.0315	53.88
	0.008	0.0210	69.25

observed in the alloys immersed in 3.5% NaCl solution (Fig. 4e). With the addition of 0.005 M tryptophan to the three solutions above, the corrosion of the aluminum alloys was greatly decreased, as shown in Fig. 4(b, d, and f). According to these experimental results, tryptophan can be safely concluded to act as an effective inhibitor in these three corrosion media, and it significantly inhibits the corrosion of aluminum alloys.

3.4 Quantum-Chemical Calculation

Figure 5(a) shows the automatically optimized geometry of the tryptophan molecule calculated by the Dmol^3 program of Material Studio 4.0. Figure 5 shows that all atoms of the indole ring are in a plane where the delocalization of π electrons exists.

The highest occupied molecular orbital (HOMO) and the lowest unoccupied molecular orbital (LUMO) surfaces of the tryptophan molecule are given in Fig. 5(b) and (c). The energies of the HOMO and LUMO of the molecule and energy gap $(\Delta E = E_{LUMO} - E_{HOMO})$ were found to be −5.075, −1.390, and 3.685 eV, respectively. The HOMO and LUMO locations in the tryptophan molecule were mostly distributed in the vicinity of the indole ring. This indicates that interactions between the metal surface and the tryptophan molecule take place over the indole ring.
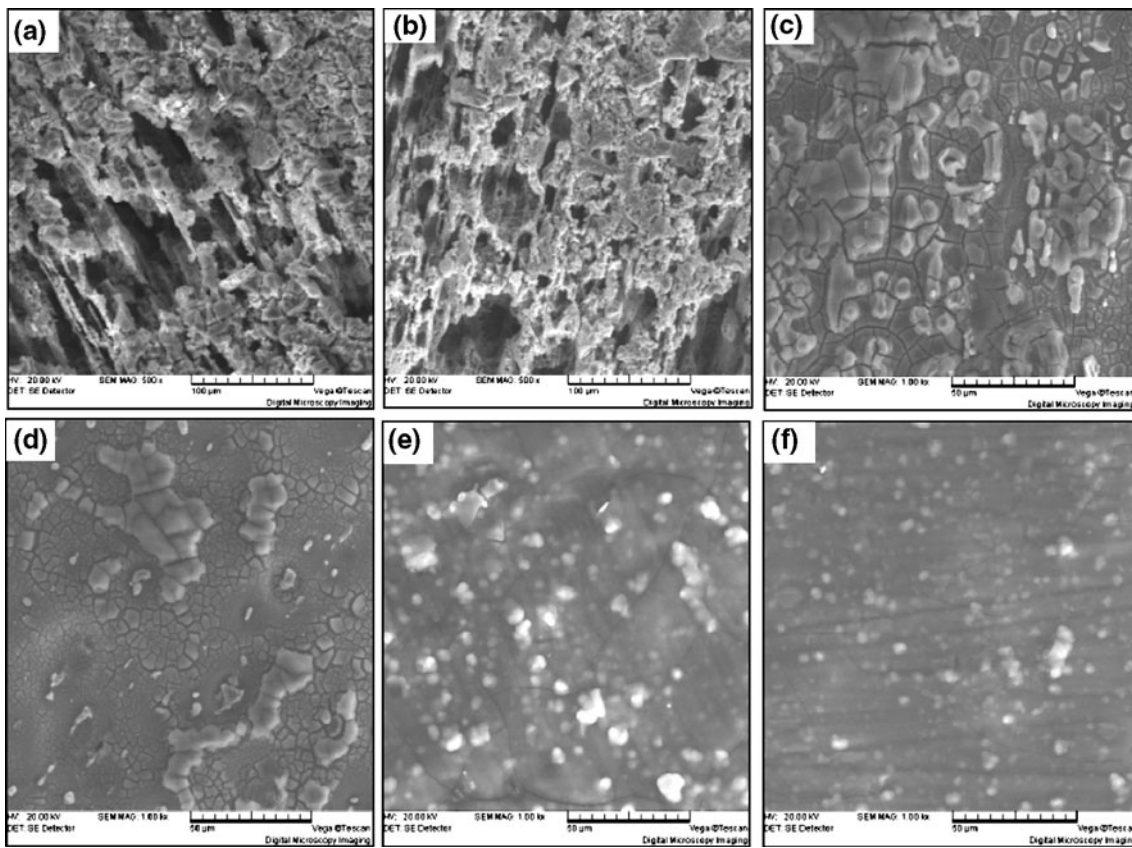
Fig. 4 SEM images of the corrosion morphology of aluminum alloy exposed to (a) 1 M HCl, (b) 1 M HCl + 0.005 M tryptophan, (c) 20% CaCl$_2$, (d) 20% CaCl$_2$ + 0.005 M tryptophan, (e) 3.5% NaCl, and (f) 3.5% NaCl + 0.005 M tryptophan
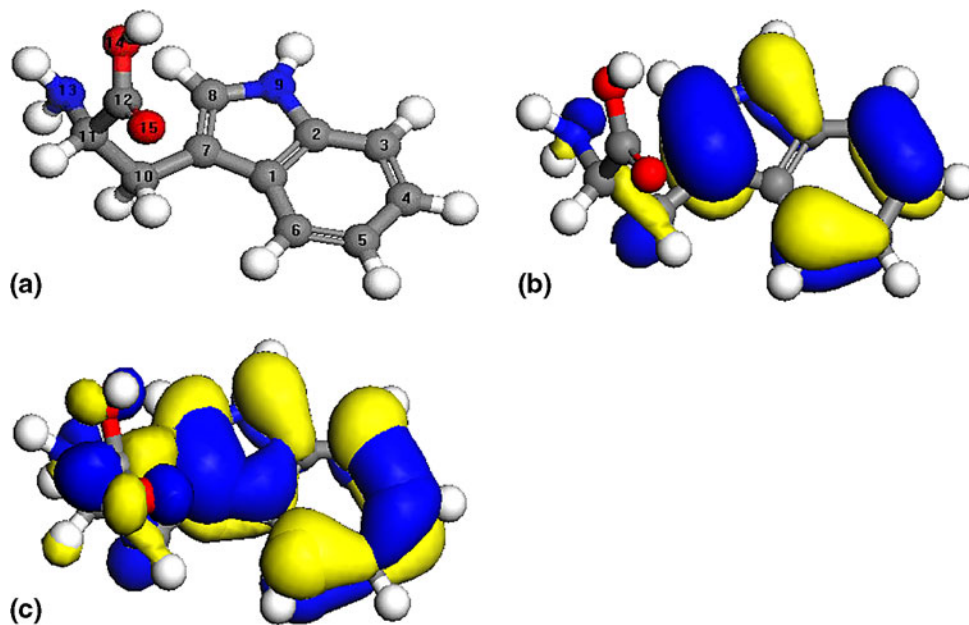

Fig. 5 (a) Optimized geometry, (b) highest occupied molecular orbital (HOMO), and (c) lowest unoccupied molecular orbital (LUMO) surfaces of the tryptophan molecule

To clarify the interaction between the adsorbent molecule and metal surface, a local type of reactivity criterion should be considered, such as the Fukui index (Ref 18). The Fukui indices for the system were determined as described by Yang and Mortier (Ref 19), and calculations for the $N + 1$ and $N - 1$ electron species at the geometry of the reference N-electron tryptophan molecule were carried out. The higher values of the condensed Fukui indices, f^- and f^+, are given

Table 3 The Fukui indices' values

Electrophilic attack (f^-)		Nucleophilic attack (f^+)	
Heteroatom	Fukui indices	Heteroatom	Fukui indices
C (7)	0.079	C (3)	0.083
C (8)	0.084	C (8)	0.068
N (9)	0.059	O (15)	0.083

in Table 3. Once the adsorbent molecule donates a charge to the metal, an analysis of the local reactivity can be performed by condensed Fukui index f^- (for an electrophile), while analysis of the adsorbent molecule that receives a charge from the metal can be performed by f^+ (for a nucleophile) (Ref 20). The value of the Fukui index indicates that C(3) and O(15) of the tryptophan molecule are the most susceptible sites when molecules undergo nucleophilic attack. The most reactive site for electrophilic attack, on the other hand, is C(8) (Table 3).

The localization of the frontier molecular orbital is complete, thus agreeing with the atom exhibiting the greatest Fukui index value. This finding indicates that tryptophan adsorbs onto metal surfaces via the indole ring.

4. Conclusion

(1) Tryptophan showed excellent inhibition against aluminum corrosion in the three corrosion media (1 M HCl, 20% $CaCl_2$, and 3.5% NaCl). The inhibition efficiency of tryptophan increased as its concentration increased, reaching 87% at a concentration of 0.008 M tryptophan.

(2) Tryptophan acts as a cathodic corrosion inhibitor in 1 M HCl solution and as an anodic corrosion inhibitor in both 20% $CaCl_2$ and 3.5% NaCl solutions.

(3) Data from the quantum-chemical calculations indicate that the interactions between the metal surface and tryptophan molecule mainly occur over the indole ring plane.

References

1. S. Wernick, R. Pinner, and P.G. Sheasby, *The Surface Treatment of Aluminum and its Alloys*, Vol 1, ASN International Finishing Publications Ltd., Teddington, UK, 1987

2. C.-h. Yu, The Analysis on Chemical Cleaning Agent in Aluminum Fin Cool-Exchanger, *Chem. Clean.*, 1999, **15**(2), p 12–16

3. D.-x. Yu, Preparation of a Normal Temperature High Efficiency Cleaner for Aluminum Slices, *Fine Chem.*, 2003, **20**(2), p 126–128

4. Q.-z. Joao, Study on the Inhibitor of SH-904 and JA-1 on Aluminum in Hydrochloric Acid Solution, *J. Sci. Teachers' Coll. Univ.*, 2004, **2**(44), p 23–25

5. N.-l. Wang and X.-b. Liu, Prevention Analysis of Salt-Spray Corrosion Coating of Aluminium Heat Exchanger, *Mech. Manag. Develop.*, 2007, **6**(3), p 33–35

6. J.-y. Zuo, *Stress Corrosion Crack*, Xi'an Jiao Tong University Press, Xi'an, 1985, p 222–225

7. Y.-l. Wang and J.-s. Wang, Corrosion Analysis of Heat Exchanger in Electric Desalter of Delay Cooking Unit, *Mater. Mech. Eng.*, 2008, **1**(32), p 81–83

8. Z. Mu and S.-w. Jing, Corrosion and Prevent of Heat Exchanger, *Large Scale Nitrogenous Fertilizer Industry*, 2008, **5**(3), p 38–40

9. A.A. El-Shafei, M.N.H. Moussa, and A.A. El-far, Inhibitory Effect of Amino Acids on Al Pitting Corrosion in 0.1 M NaCl, *J. Appl. Electrochem.*, 1997, **27**(9), p 1075–1078

10. X.-k. Yang, Preparation of the Pickling Inhibitor of Complex Amino Acid, *New Technol. New Process*, 2002, **10**, p 39–40

11. H. Ashassi-Sorkhabi, M.R. Majidi, and K. Seyyedi, Investigation of Inhibition Effect of Some Amino Acids Against Steel Corrosion in HCl Solution, *Appl. Surf. Sci.*, 2004, **225**(1/4), p 176–185

12. E.E. Oguzie, Y. Li, and F.H. Wang, Corrosion Inhibition and Adsorption Behavior of Methionine on Mild Steel in Sulfuric Acid and Synergistic Effect of Iodide Ion [J], *J. Colloid Interface Sci.*, 2007, **310**(1), p 90–98

13. M.A. Kiani, M.F. Mousavi, S. Ghasemi, M. Shamsipur, and S.H. Kazemi, Inhibitory Effect of Some Amino Acids on Corrosion of Pb-Ca-Sn Alloy in Sulfuric Acid Solution, *Corros. Sci.*, 2008, **50**(4), p 1035–1045

14. Metal Materials—Uniform Corrosion—Methods of Laboratory Immersion Testing. GB10124-88, Chinese National Standard, 1990, p 119–126

15. S.-z. Song, Electrochemical Methods for Corrosion Investigation[M], Chemical Industry Press, Beijing, 1988, p 164–165

16. I. Epelboin and M. Keddam, Faradic Impedance: Diffusion Impedance and Reaction Impedance, *Electrochem. Soc.*, 1970, **117**, p 1052–1061

17. M. Keddam, O.R. Mattos, and H. Takenouti, Reaction Model for Iron Diffusion Studied by Electrode Impedance, *Electrochem. Soc.*, 1959, **55**, p 1562–1586

18. R.G. Parr and W. Yang, Density Functional Approach to the Frontier-electron Theory of Chemical Reactivity, *J. Am. Chem. Soc.*, 1984, **106**(14), p 4049–4050

19. W. Yang and W.J. Mortier, The Use of Global and Local Molecular Parameters for the Analysis of the Gas-phase Basicity of Amines, *J. Am. Chem. Soc.*, 1986, **108**(19), p 5708–5713

20. B. Gómez, N.V. Likhanova, M.A. Domínguez-Aguilar, R. Martínez-Palou, A. Vela, and J.L. Gazquez, Quantum Chemical Study of the Inhibitive Properties of 2-Pyridyl-Azoles, *J. Phys. Chem. B*, 2006, **110**(18), p 8928–8937